

Dispersive Excitations in the High-Temperature Superconductor $\text{La}_{2-x}\text{Sr}_x\text{CuO}_4$

N. B. Christensen,¹ D. F. McMorrow,^{1,2,3} H. M. Rønnow,^{4,5} B. Lake,⁶ S. M. Hayden,⁷ G. Aeppli,² T. G. Perring,³
M. Mangkorntong,⁸ M. Nohara,⁸ and H. Takagi⁹

¹Materials Research Department, Risø National Laboratory, 4000 Roskilde, Denmark

²London Centre for Nanotechnology and Department of Physics and Astronomy, University College London,
London WC1E 6BT, United Kingdom

³ISIS Facility, Rutherford Appleton Laboratory, Chilton, Didcot OX11 0QX, United Kingdom

⁴Laboratory for Neutron Scattering, ETH Zürich & PSI Villigen, CH-5232 Villigen PSI, Switzerland

⁵The James Franck Institute and Department of Physics, University of Chicago, Illinois 60637, USA

⁶Department of Physics, Oxford University, Oxford, OX1 3PU, United Kingdom

⁷H.H. Wills Physics Laboratory, University of Bristol, Bristol BS8 1TL, United Kingdom

⁸Institute for Solid State Physics, University of Tokyo, Tokyo 113-8656, Japan

⁹Department of Advanced Materials Science, University of Tokyo, Kashiwa 277-8651, Japan
(Received 17 March 2004; published 28 September 2004)

High-resolution neutron scattering experiments on optimally doped $\text{La}_{2-x}\text{Sr}_x\text{CuO}_4$ ($x = 0.16$) reveal that the magnetic excitations are dispersive. The dispersion is the same as in $\text{YBa}_2\text{Cu}_3\text{O}_{6.85}$, and is quantitatively related to that observed with charge sensitive probes. The associated velocity in $\text{La}_{2-x}\text{Sr}_x\text{CuO}_4$ is only weakly dependent on doping with a value close to the spin-wave velocity of the insulating ($x = 0$) parent compound. In contrast with the insulator, the excitations broaden rapidly with increasing energy, forming a continuum at higher energy and bear a remarkable resemblance to multiparticle excitations observed in 1D $S = 1/2$ antiferromagnets. The magnetic correlations are 2D, and so rule out the simplest scenarios where the copper oxide planes are subdivided into weakly interacting 1D magnets.

DOI: 10.1103/PhysRevLett.93.147002

PACS numbers: 74.72.Dn, 61.12.-q, 74.25.Ha

The defining properties of any particle or wavelike excitation are the dimensionality of the space in which it moves and its dispersion. Conventional magnets host spin waves, which are coherently precessing deviations of the spins from their equilibrium, ordered configuration. The antiferromagnetic (AF), insulating parents of the high-temperature, CuO_2 based superconductors are no exception to this rule [1]. An important question is what happens to the magnetic excitations upon chemical doping to produce metals and superconductors. Here we describe experiments on $\text{La}_{2-x}\text{Sr}_x\text{CuO}_4$ (LSCO) which reveal that the magnetic excitations are in fact dispersive and appear, at least at low energies, to be two-dimensional (2D). However, they are not derived from propagating excitations in the manner of ordinary spin waves. We show how these dispersive spin excitations bear a quantitative relation to those in the $\text{YBa}_2\text{Cu}_3\text{O}_{6+x}$ (YBCO) family [2,3], and more astonishingly, to charge sensitive measures of electronic excitations [4,5]. This discovery clearly establishes the notion of universality amongst the different cuprate families, and will greatly simplify the theory for this highly varied class of complex materials.

The technique chosen is inelastic neutron scattering, which measures the spin excitation spectrum, $\chi''(\mathbf{Q}, \omega)$, as a function of both momentum $\hbar\mathbf{Q}$ and energy $\hbar\omega$. Many neutron experiments have been performed on the superconducting (SC) cuprates, and it is fair to ask why another is needed. The reason is that the new MAPS

spectrometer at ISIS, UK finally can provide the long sought for definitive results by offering global momentum and energy surveys with momentum resolution as small as 0.02 \AA^{-1} rather than the more typical 0.1 \AA^{-1} . Nine single crystals of $\text{La}_{1.84}\text{Sr}_{0.16}\text{CuO}_4$ (total mass of 18.7 g, $T_c = 38.5 \text{ K}$) grown by the floating zone method were coaligned. The sample was mounted with the SC planes perpendicular to the incident beam of neutrons, selected to have an energy of 55 meV. Data were collected at 10 and 40 K, and were converted to $\chi''(\mathbf{Q}, \omega)$ in absolute units of $\mu_B^2 \text{ eV}^{-1}$ per formula unit (f.u.).

The undoped parent La_2CuO_4 displays commensurate AF order, giving a diffraction peak at $\mathbf{Q} = (\pi, \pi)$ [Fig. 1(a)]. Upon doping, the peak splits into four incommensurate (IC) spots [6,7] reflecting the fact that in real space, the AF correlations have become modulated with a period inversely related to $\delta\pi$, the distance in reciprocal space from (π, π) . In one very popular model [8–10], the modulation is due to a tendency of the CuO_2 planes to break into stripes creating 1D magnets. If these magnets were truly independent of each other, they would give rise to perpendicular streaks of scattering. Since there are two equivalent directions to choose from, a typical sample would produce orthogonal streaks passing through (π, π) [Fig. 1(b)]. Only an internal modulation along each stripe, as occurs for spin 1/2 chains doped with holes or in an external magnetic field [11], can produce IC features in neutron scattering images, such as the crossing of streaks from diagonal stripes [Fig. 1(c)].

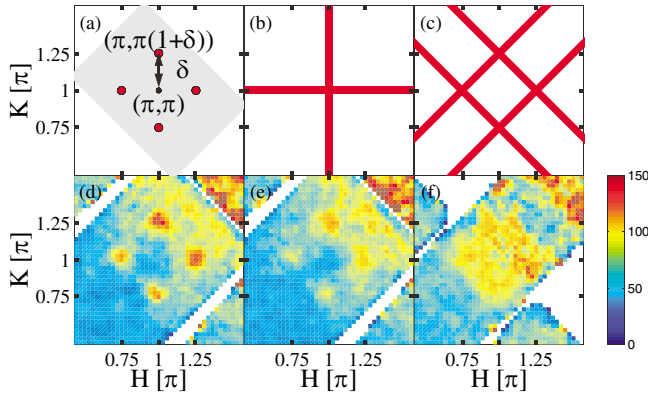


FIG. 1 (color online). (a)–(c) 2D reciprocal space indicating the diffraction patterns for different scenarios of the magnetic correlations. (d)–(f) Images from MAPS of $\chi''(\mathbf{Q}, \omega)$ for LSCO $x = 0.16$. Color scale: intensity in units of $\mu_B^2 \text{ eV}^{-1} \text{ f.u.}^{-1}$. (d) and (f) $T = 10 \text{ K}$ in the SC phase for $\hbar\omega = 10$ and 30 meV , respectively. (e) $T = 40 \text{ K}$ in the normal phase at 10 meV .

Figure 1(d)–1(f) displays images of $\chi''(\mathbf{Q}, \omega)$ for $\text{La}_{1.84}\text{Sr}_{0.16}\text{CuO}_4$, produced directly from the raw data without performing any background subtraction. They are the first to afford complete, high isotropic resolution coverage of reciprocal space for superconducting LSCO, and directly reveal a very important fact. In the SC phase at $T = 10 \text{ K}$ and at low energies [Fig. 1(d) $\hbar\omega = 10 \text{ meV}$], the magnetic response starts out as sharp, isotropic peaks at the quartet of IC positions [Fig. 1(a)], with essentially no scattering at $\mathbf{Q} = (\pi, \pi)$ and no evidence for the streaks sketched in Fig. 1(b) or 1(c). The isotropy of the peaks and absence of obvious streaks implies [9,10] that the magnetic correlations are 2D, which immediately rules out any scenario based on a naive subdivision of the material into weakly coupled magnetic stripes. Until now, the extent of this isotropy has not been clear because data have been collected using instruments with highly anisotropic resolution functions. If a stripe picture is used to interpret our data, there must be strong interstripe as well as intrastripe exchange coupling.

Warming to just above T_c [Fig. 1(e)], the IC peaks weaken as spectral weight is shifted to fill the spin gap at lower energy [7]. We gain dramatic new knowledge by going to 30 meV [Fig. 1(f)], where we see that the peaks are no longer well defined. Instead, the scattering appears more as a “box” surrounding (π, π) , and there is now also substantial scattering at (π, π) .

In Fig. 2, we examine the data in more detail by looking at constant-energy cuts through the images in Fig. 1. Figure 2(a) displays the IC peaks at $E = 10 \text{ meV}$, and it is evident from Fig. 2(b) that at this energy, the sides of the IC box are very weak. By increasing E to 30 meV , it is clear that the response has moved in towards (π, π) (Fig. 1), meaning that it is dispersive. In addition, the peaks lose definition—the corners [Fig. 2(c)] are now no sharper than the sides of the box [Fig. 2(d)], and both

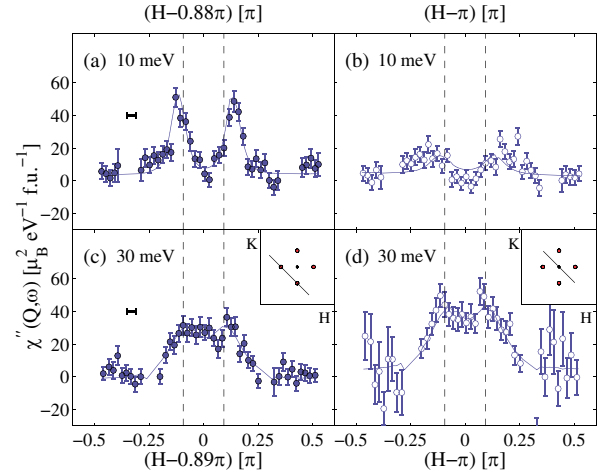


FIG. 2 (color online). Constant-energy cuts through $\chi''(\mathbf{Q}, \omega)$ from MAPS for LSCO $x = 0.16$ at $T = 10 \text{ K}$. The scan trajectory is transverse as shown in the insets. Solid lines: fits to the model discussed in the text. Vertical dashed lines: fitted peak positions at 30 meV . Horizontal bars in (a) and (c) represent the instrumental resolution (FWHM). Using the wide reciprocal space coverage of MAPS, it was possible to determine accurately the background at positions away from the magnetic scattering. This background has been subtracted from the data shown here.

we broadened so that there is considerable scattering even at (π, π) . This transition to broader, continuum-like scattering implies that we are not dealing with well-defined bosonic modes of a quantum spin liquid or AF. A key result of our work, namely, that the IC peaks disperse and cannot be due to conventional propagating modes, is thus seen by straightforward display of the data.

We analyzed the momentum-dependent images using

$$\chi''(\mathbf{Q}, \omega) = \sum_{\delta} \frac{\chi_{\delta}(\omega) \kappa^4(\omega)}{[\kappa^2(\omega) + [\mathbf{Q} - \mathbf{Q}_{\delta}(\omega)]^2]^2}, \quad (1)$$

where $\kappa(\omega)$ is an inverse correlation length, and the sum runs over the four IC positions. A good description of the data was obtained by convoluting the above line shape with the full instrumental resolution function and fitting it to the data (see Fig. 2). From this analysis, values were obtained of the incommensurability δ , inverse correlation length $\kappa(\omega)$, and intensity $\chi_{\delta}(\omega)$ of the magnetic fluctuations. The values of δ are plotted in Fig. 4(a). It is as apparent from the fits, as from the raw data, that the peaks in the response move closer to $\mathbf{Q} = (\pi, \pi)$ and broaden with increasing energy. No change of δ is observed on entering the SC state. To emphasize that dispersion of the IC mode is a generic feature of LSCO, we also show data taken using MAPS for an underdoped LSCO sample, $x = 0.10$, where the initial incommensurability is lower, but the velocity is the same. What is even more remarkable is that the velocity associated with dispersion of the nonpropagating spin excitations seen

here for the metals is the same (~ 1 eV \AA) as that for the propagating spin waves in the parent insulator [1]. Figure 4(b) shows the peak width, which above 20 meV is indistinguishable in the normal and SC phases; at lower energies, the excitations become more coherent in the SC state [7].

Figure 3(a) displays peak intensities, including data from the same crystals obtained at the RITA spectrometer, Risø, Denmark. As observed previously, superconductivity redistributes the spectral weight from energies below the spin gap $\Delta = 7$ meV, to higher energies [7]. What is new is that we are able now to see the full extent of the redistribution. The net effect is to produce a peak in $\chi''(\mathbf{Q}, \omega)$ centered at 12 ± 2 meV, although the redistribution takes place for energies up to about 30 meV. Figure 3(b) presents the local susceptibility $\chi''(\omega)$ calculated by integrating the response over the 2D Brillouin zone. In the SC phase, $\chi''(\omega)$ is peaked at 18 ± 2 meV, with a half width at half maximum of 12 ± 2 meV. The normal state mean-squared fluctuating moment [12], calculated from $\chi''(\omega)$ up to 40 meV, is $\langle m^2 \rangle = 0.062 \pm 0.005 \mu_B^2(\text{CuO}_2)^{-1}$ and is unchanged on cooling through T_c . In other words, the spectral weight removed by the opening of the spin gap is preserved and merely shifted to higher energy. A similar shift of spectral weight leads to the formation of a commensurate “resonance” at $\mathbf{Q} = (\pi, \pi)$ in lightly doped $\text{YBa}_2\text{Cu}_3\text{O}_{6+x}$ [12,13]. In the case of LSCO, the amount of spectral weight shifted is $\delta \langle m^2 \rangle = 0.010 \pm 0.005 \mu_B^2(\text{CuO}_2)^{-1}$, of the same order as $\delta \langle m^2 \rangle = 0.03 \mu_B^2(\text{CuO}_2)^{-1}$, in the resonance of $\text{YBa}_2\text{Cu}_3\text{O}_{6.6}$ [12]. That the spectral weight in LSCO is

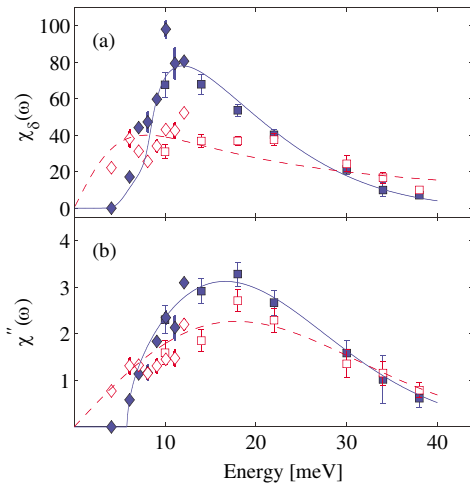


FIG. 3 (color online). (a) Energy dependence of $\chi_\delta(\omega)$, the fitted peak intensity of $\chi''(\mathbf{Q}, \omega)$ at \mathbf{Q}_δ for LSCO $x = 0.16$ in units of $\mu_B^2 \text{eV}^{-1} \text{f.u.}^{-1}$ [see Eq. (1)]. Superconducting phase, filled symbols; normal phase, open symbols. MAPS data, squares; triple-axis data, diamonds. (b) Local susceptibility $\chi''(\omega)$. Symbols as in (a). Lines are guides to the eye. The region 24–28 meV was found to be strongly contaminated by phonon scattering and was not analyzed.

conserved already up to 40 meV makes the existence of the long sought after higher frequency *commensurate* resonance as in YBCO [14–16] very improbable.

It has often been stated that the IC fluctuations in LSCO are dispersionless and a pathology of this single layer material [3,6]. We argue here that this view is incorrect, even though at first glance YBCO displays a quite different magnetic response. Below T_c , $\chi''(\mathbf{Q}, \omega)$ is dominated by a resonance peak at $\mathbf{Q} = (\pi, \pi)$ ($E_{\text{res}} = 41$ meV in the case of optimal doping) [14–16]. Subsequent work revealed that at lower energies, $E < E_{\text{res}}$, the response becomes IC [2,3,17]. Here we have discovered that the IC response in LSCO is dispersive and remarkably similar to that of $\text{YBCO}_{6.85}$ as shown in Fig. 4(c). The main difference between the two systems is that the spectral weight redistribution in LSCO takes place well below the energy where the IC modes begin to merge [Fig. 4(d)]. In YBCO, the larger spin gap results in spectral weight being pushed into the region where the IC modes merge, forming a sharp peak-like response.

While our data resemble those for YBCO, they differ from those for conventional magnets, even with long-period order. For example, $\text{La}_{1.69}\text{Sr}_{0.31}\text{NiO}_4$ [18] displays two sharply defined modes emanating symmetrically from each IC wave vector as indicated by the solid lines in Fig. 4(d). More recently, a study [19] of nonsuperconducting $\text{La}_{1.875}\text{Ba}_{0.125}\text{CuO}_4$ reported asymmetric dispersion, but did not specifically address the line shape, and

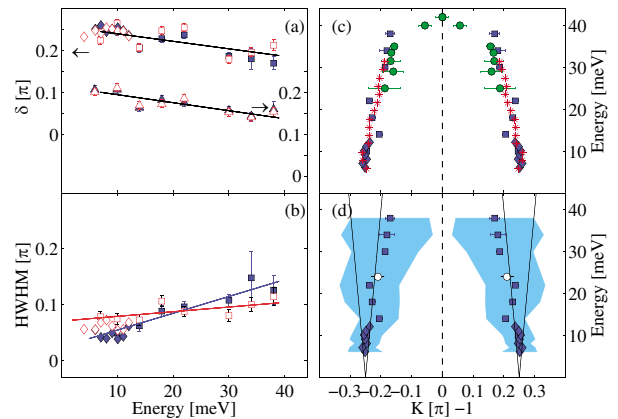


FIG. 4 (color online). (a) Incommensurability δ in LSCO. Squares: MAPS, LSCO $x = 0.16$. Triangles: MAPS, LSCO $x = 0.10$. Diamonds: RITA, LSCO $x = 0.16$. Filled symbols, superconducting phase; open symbols, normal state. (b) Energy dependence of the peak half width. Symbols as in (a). (c) Comparison of δ for the superconducting phases of optimally doped LSCO symbols as in (a) and $\text{YBCO}_{6.85}$ (circles, [17]), and half the wave vector of the electronic excitations (stars, [4]) observed along the (1,0) direction in $\text{Bi}_2\text{Sr}_2\text{CaCu}_2\text{O}_{8+\delta}$ using STM. (d) Dispersion of the excitations in LSCO. Shaded regions represent the fitted FWHM. Solid lines show the spin-wave velocity of La_2CuO_4 with $J = 156$ meV [1]. Open circle: $\text{YBCO}_{6.6}$ [16].

provided no information on any broadening at low energies. In contrast, our high-resolution experiments show that the magnetic excitations disperse in only one direction (inwards), and broaden with increasing energy as rapidly as they disperse [Fig. 4(d)]. This means that we are not dealing with propagating spin-wave modes of the type found in conventional magnets.

Instead, our observed response is best described as resulting from a continuum of excitations, indicating that the neutron does not excite the fundamental quasiparticles of the system, but rather coherent pairs, quartets and so on, of quasiparticles. There are several candidates for the underlying quasiparticles. In the ordinary theory of metals, the underlying particles are simply electrons and the multiparticle excitations, which neutron scattering would observe are correlated electron-hole pairs. Many theories attempt to explain cuprate spin fluctuations in terms of propagating electrons and holes described by an underlying band structure [20–22]. However, we lack a single model which describes the remarkable robustness of the velocity with respect to doping [Fig. 4(a)], the absence of measurable dispersion in the spin gap [7], and the universality of the observed response between the bilayer and single layer materials [Fig. 4(c)]. A second possibility for the underlying excitations is suggested by returning to the concept of spin-charge separation introduced to the cuprates almost immediately after the discovery of high- T_c superconductivity [23,24]. Here the fundamental quasiparticles are no longer electrons, carrying spin $1/2$ and charge $-e$; instead, they are charge neutral objects, spinons, carrying spin $1/2$, and spinless objects, holons, carrying charge $+e$. While this picture has been verified in 1D [11,25], its applicability in 2D has been more controversial. Spin-charge separation in the cuprates could occur by subdivision into 1D chains [26], as suggested by the simplest stripe picture [9,10], or via the effect of competing interactions on 2D quantum systems [27,28]. Further work is required to differentiate between these two possibilities. Both descriptions imply proximity to a quantum critical point, which naturally leads to a magnetic response dominated by nonpropagating modes, and has provided a framework for understanding the low-frequency properties of an LSCO sample with $x = 0.14$ [29], close to the special filling fraction $x = 1/8$.

We end by pointing out a correlation between our data and recent STM experiments which have observed dispersing charge quasiparticles. Specifically, the stars in Fig. 4(c) represent the position along $[1,0]$ of the most obvious IC peak from STM data (positive bias) for “as grown” $\text{Bi}_2\text{Sr}_2\text{CaCu}_2\text{O}_{8+\delta}$ [4]. Within the conventional band theory of ordinary paramagnetic metals, the loci of the charge and spin responses in Q - E space should coincide. This is actually not the case—the STM wave vectors, when divided by a factor of 2, line up with the

neutron data. This factor of 2 is of course familiar from the static order seen in conventional magnets [8,30]. It is quite astonishing that, once this factor of 2 is included, the spin and electronic response functions measured by neutrons and STM for different materials display nearly identical dispersions. The question remains open as to whether this correlation reflects a profound and direct relationship between what is being probed by the two techniques or is coincidental.

We acknowledge stimulating discussions with B. Møller Andersen, S. Davis, S. Chakravarty, T. Giammarchi, P. Hedegård, S. Kivelson, K. Lefmann, and J. Mesot, and are especially grateful to T. Rosenbaum for his support through the National Science Foundation Grant No. DMR-0114798. Work in London was supported by a Wolfson Royal Society Research Merit Award and the Basic Technology program of the UK research councils, while that in Risø was supported by the Danish Natural Science Council via DanScatt and the Danish Technical Research Council under the Framework Program on Superconductivity.

-
- [1] S. M. Hayden *et al.*, Phys. Rev. Lett. **67**, 3622 (1991).
 - [2] P. Dai *et al.*, Phys. Rev. B **63**, 054525 (2001).
 - [3] P. Bourges *et al.*, Science **288**, 1234 (2000).
 - [4] J. E. Hoffman *et al.*, Science **297**, 1148 (2002).
 - [5] K. McElroy *et al.*, Nature (London) **422**, 592 (2003).
 - [6] K. Yamada *et al.*, Phys. Rev. B **57**, 6165 (1998).
 - [7] B. Lake *et al.*, Nature (London) **400**, 43 (1999).
 - [8] J. M. Tranquada *et al.*, Nature (London) **375**, 561 (1995).
 - [9] J. Zaanen *et al.*, Philos. Mag. B **81**, 1485 (2001).
 - [10] S. A. Kivelson *et al.*, Rev. Mod. Phys. **75**, 1201 (2003).
 - [11] A. M. Tselik, *Quantum Field Theory in Condensed Matter Physics* (Cambridge University Press, Cambridge, England, 1996).
 - [12] P. Dai *et al.*, Science **284**, 1344 (1999).
 - [13] C. Stock *et al.*, Phys. Rev. B **69**, 014502 (2004).
 - [14] J. Rossat-Mignod *et al.*, Physica C (Amsterdam) **185**, 86 (1991).
 - [15] H. F. Fong *et al.*, Phys. Rev. Lett. **78**, 713 (1997).
 - [16] H. A. Mook *et al.*, Nature (London) **395**, 580 (1998).
 - [17] H. M. Rønnow *et al.*, Institut Laue-Langevin, Annual Report (2000), p. 18.
 - [18] P. Bourges *et al.*, Phys. Rev. Lett. **90**, 147202 (2003).
 - [19] J. M. Tranquada *et al.*, Nature (London) **429**, 534 (2004).
 - [20] Y.-J. Kao *et al.*, Phys. Rev. B **61**, 11898 (2000).
 - [21] M. R. Norman, Phys. Rev. B **61**, 14751 (2000).
 - [22] A. V. Chubukov *et al.*, Phys. Rev. B **63**, 180507 (2001).
 - [23] P. W. Anderson, Science **235**, 1196 (1987).
 - [24] D. S. Rokhsar and S. A. Kivelson, Phys. Rev. Lett. **61**, 2376 (1988).
 - [25] D. A. Tennant *et al.*, Phys. Rev. Lett. **70**, 4003 (1993).
 - [26] E. Dagotto and T. M. Rice, Science **271**, 618 (1996).
 - [27] R. Coldea *et al.*, Phys. Rev. B **68**, 134424 (2003).
 - [28] P. A. Lee and N. Nagaosa, Phys. Rev. B **46**, 5621 (1992).
 - [29] G. Aeppli *et al.* Science **278**, 1432 (1997).
 - [30] O. Zachar *et al.*, Phys. Rev. B **57**, 1422 (1998).